

# Direct reading measurement of absorbed dose with plastic scintillators— The general concept and applications to ophthalmic plaque dosimetry

D. Flühs, M. Heintz, F. Indenkampen, and C. Wieczorek

*Klinische Strahlenphysik, Strahlentherapie, Universitätsklinikum Essen, Hufelandstrasse 55, D-45122 Essen, Germany, and Institut für Physik, Universität Dortmund, Otto-Hahn-Strasse 4, D-44221 Dortmund, Germany*

H. Kolanoski

*Institut für Physik, Humboldt-Universität zu Berlin, Platanenallee 6, D-15738 Zeuthen, Germany*

U. Quast

*Klinische Strahlenphysik, Strahlentherapie, Universitätsklinikum Essen, Hufelandstrasse 55, D-45122 Essen, Germany*

(Received 9 January 1995; accepted for publication 23 October 1995)

We have developed dosimeters based on plastic scintillators for a variety of applications in radiation therapy. The dosimeters consist basically of a tissue-substituting scintillator probe, an optical fiber light guide, and a photomultiplier tube. The background light generated in the light guide can be compensated by a simultaneous measurement of the light from a blind fiber. Plastic scintillator dosimeters combine several advantageous properties which render them superior to other dosimeter types for many applications: minimal disturbance of the radiation field because of the homogeneous detector volume and the approximate water equivalence; no dependence on temperature and pressure (under standard clinical conditions) and angle of radiation incidence; no high voltage in the probe; high spatial resolution due to small detector volumes; direct reading of absorbed doses; and a large dynamical range. The high spatial resolution together with direct reading make these detectors suitable for real-time 3-D dosimetry using multi-channel detector systems. Such a system has been developed for eye plaque dosimetry and successfully employed for dosimetric treatment optimization. The plaque optimization can be performed by dosimetric measurements for the individual patient ("dosimetric treatment planning"). The time consumption for this procedure is less than for a physically correct computer-based therapy planning, e.g., by means of a Monte Carlo simulation. © 1996 American Association of Physicists in Medicine.

Key words: plastic scintillator dosimetry, tissue equivalence, multi-channel dosimeters, eye plaque dosimetry

## I. INTRODUCTION

An ideal detector for the measurement of the absorbed dose does not disturb the physical conditions. This ideal situation can be closely approximated by plastic scintillator probes because such probes have a homogeneous sensitive volume with approximate water equivalence in density and atomic composition.

Due to their high sensitivity, scintillation detectors can be designed with probe volumes as small as 1 mm<sup>3</sup> or even less. This renders them suitable for applications where a high spatial resolution is needed (small structures or steep dose gradients). Compared to thermo-luminescence detectors (TLD), which have been used for such applications in the past, scintillation detectors offer the great advantage that they can be read out directly. The direct reading of absorbed doses and dose rates opens wide applications for real time control of radiation treatment and detailed mapping of radiation fields in two and three dimensions.

Although plastic scintillators have been manufactured for decades, they had not found a wider application in dosimetry before flexible optical fibers with sufficient transmission of scintillation light and with the possibility of simultaneous

Cerenkov compensation became available. First attempts to use scintillators for dosimetry have already been reported back in the sixties and seventies, e.g., in the publications of Meisberger *et al.*,<sup>1</sup> O'Foghludha,<sup>2</sup> and Schmidt.<sup>3</sup> However, applications of scintillation dosimeters in the clinical routine have only recently been described in the literature.<sup>4-6</sup>

A problem which needs special attention is the generation of Cerenkov and luminescence light in the light guides.<sup>7-10</sup> A solution for this problem of background light was described by Beddar *et al.*<sup>4,5</sup> and by Flühs *et al.*<sup>6,11</sup> Using multi-fiber light guides where some of the fibers are not connected to the scintillator (Fig. 1), the background light can be measured simultaneously and be subtracted. We have successfully employed such dosimeter systems with Cerenkov compensation for external beam photon dosimetry.<sup>6,11,12</sup>

In this article we describe the general concept and the physical and technical principles of plastic scintillator dosimetry and report on our experience with complete systems emphasizing the development of multi-detector systems. Such systems employ multi-channel photomultiplier tubes (PMT) and computer-controlled readout for real-time three-dimensional dose measurement.

The broad range of applications in clinical dosimetry will

87.53.05  
87.55.07

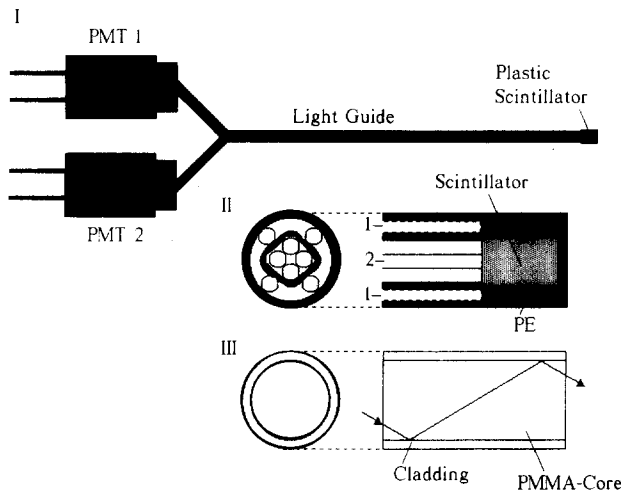


FIG. 1. (I) Diagram of the scintillation dosimeter system. (II) Cross section of the probe with the plastic scintillator embedded in a flexible polyethylene (PE) tube. Distribution of the light guide fibers: (1) background fiber, and (2) signal light fiber. (III) Cross section of a single fiber, showing the core and cladding.

be discussed. As an example, we demonstrate the advantages of plastic scintillators for ophthalmic plaque dosimetry. Fast documentation of dose distribution allows optimization of the plaque design (dosimetric treatment planning) as well as quality assurance in the clinical routine. We show the development of iodine applicators which provide a better sparing of radiosensitive structures in the eye region.

## II. THE GENERAL CONCEPT OF PLASTIC SCINTILLATOR DOSIMETRY

### A. Physical properties of the scintillator

#### 1. Selection of a suitable scintillator

In selecting the scintillator type for dosimetry, one has to consider not only dosimetric properties such as water equivalence but also practical aspects such as radiation hardness and easy handling. We tested seven types of plastic scintillators and chose the NE 102A of the company Nuclear Enterprise, a well-investigated and widely used material (see references in the NE catalogue, Nuclear Enterprise Technology, Ltd., Reading, UK, 1993). The NE 102A is also available in the form of cladded fibers (Fig. 1). These can be cut into small pieces, thus enabling easy preparation of small detector volumes.

#### 2. Dosimetric properties—energy behavior and dose proportionality of the light yield

The physical properties of the chosen scintillator NE 102A are summarized in Table I. With a density of  $1.032 \text{ g/cm}^3$  and the composition of light atoms (hydrogen and carbon), it is almost water equivalent for most electron and photon energies important for clinical dosimetry.

Figure 2 shows the mass stopping powers and the mass absorption coefficients of polyvinyltoluene (PVT), the NE 102A base material. The small amount of additives in NE

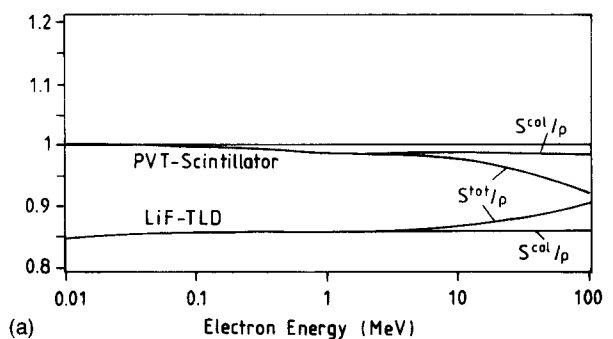
TABLE I. Physical properties of the plastic scintillator NE 102A (Scintillation Materials—Nuclear Enterprise Technology Ltd., Reading, UK, 1993).

Base:	Polyvinyltoluene
Density:	$1.032 \text{ g/cm}^3$
Softening point:	$70^\circ \text{C}$
Refractive index:	1.58
Light attenuation length:	250 cm
Light output (% anthracene):	65
Decay constant of main component:	2.4 ns
Pulse width FWHM:	2.7 ns
Wavelength of maximum emission:	423 nm
Electron density:	$3.39 \cdot 10^{23} \text{ cm}^{-3}$ (water: $3.34 \cdot 10^{23} \text{ cm}^{-3}$ )
No. of C atoms per $\text{cm}^3$ :	$4.78 \cdot 10^{22}$
No. of H atoms/No. of C atoms:	1.104

102A is negligible for this discussion. The values for the common TLD material LiF in Fig. 2 are given for comparison.

For electron energies between 10 keV and 100 MeV, the collision mass stopping power<sup>13</sup> in PVT and water does not differ by more than 2% [Fig. 2(a)]. Above 3 MeV the increasing effect of the radiative contribution causes deviations in the total mass stopping power. Its influence on relative dose measurements, however, is estimated to be less than 1%. Similarly, for photon energies between 150 keV and 2 MeV, where the Compton effect dominates, the ratio of the

Mass-Stopping Power relative to Water



Mass-Absorption Coefficient relative to Water

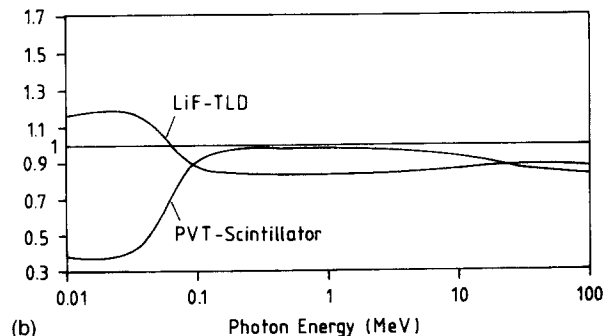


FIG. 2. (a) Mass-stopping powers (Ref. 13) of PVT (scintillator) and LiF (TLD) normalized to the mass-stopping power of water. (b) Mass-absorption coefficients (Refs. 14 and 15) of PVT (scintillator) and LiF (TLD) normalized to the mass-absorption coefficient of water.

mass absorption coefficients<sup>14,15</sup> for PVT and water differs only 2%–3% from the value 1 [Fig. 2(b)]. The scintillator contains practically no elements with a nuclear charge  $Z$  larger than 6. Thus, pair production ( $\sim Z^2$ ) diminishes the ratio of the absorption coefficients by 10% from 2 to 20 MeV, while the photo effect ( $\sim Z^{4.6}$ ) causes a steep decrease by 60% at energies from 120 keV down to 30 keV. Below 30 keV the ratio remains about constant with the attenuation in PVT being about half of that in water. This opens a window for the dosimetry of <sup>125</sup>I and <sup>103</sup>Pd sources.

A linear relation between the absorbed electron energy and the light output of the scintillator is a basic condition for dose proportionality, since in electron as well as photon beams the energy is finally deposited via energy loss of electrons. For NE 102A this holds for electron energies above 100 keV.<sup>16,17</sup> Several studies have dealt with the problem of linearity of the light yield for low-energy electrons. Horrocks<sup>18</sup> performed measurements with a toluene-based scintillator solution (similar to NE 102A). For electron energies above 80 keV he stated a linear relation between energy and light yield. Below 80 keV he observed a nonlinear relation with an offset of a few keV when extrapolating to zero signal. Kausch-Blecken von Schmeling<sup>19</sup> measured the light yield electrons with energies from 1–12 keV in NE 102. The result was a linear relation with an energy offset of 2 keV. In the discussion he pointed out that due to the small penetration depth of such electrons in the plastic (in the order of  $\mu\text{m}$ ) surface effects might dominate the measurements. Surface effects can be avoided by using low-energy photons. Meyerott *et al.*<sup>20</sup> used photon energies between 1 and 10 keV for their investigations. They stated a linear relation with an offset of 0.5 keV, in another setup the curve met the origin.

These results suggest a maximal systematical error of 1.5%–2.5% due to nonlinearities for relative dose measurements of  $\gamma$  rays and fluorescence x rays in the <sup>125</sup>I energy range of 20–35 keV. In practice, we checked these estimations by comparing scintillator and TLD measurements in iodine eye plaques (see Sec. III D).

### 3. Direction, pressure, temperature independence, and radiation hardness

The plastic NE 102A has no preferred orientation of its internal structure. Thus, its light yield does not depend on the direction of incidence of the radiation. The light output is neither affected by normal variations of the atmospheric pressure, nor by changes of the temperature between 15 °C and 45 °C. The independence of temperature was checked by dose measurements in water of different temperature.

The radiation hardness of a scintillator depends very sensitively on the additives to the base material. It does not only change from one type to another, but also for different deliveries of the same type.<sup>21</sup> The sufficiently high radiation hardness of NE 102A was verified by exposing a scintillator and a light guide (Crofon mono-fiber) to the radiation of a <sup>137</sup>Cs source over about one year.<sup>11</sup> An accumulated total dose of 1600 Gy did not change the absolute light output within the

accuracy of 3%. Similar results were reported by Beddar *et al.*<sup>4</sup>

### B. The light guide

As light guide, we have chosen the fiber CXKG of the manufacturer Toray with a diameter of 265  $\mu\text{m}$  whose core is made of PMMA and which has a 10- $\mu\text{m}$ -thick cladding of a fluoropolymere. The fiber transmits light between 400 and 700 nm with an attenuation of less than 500 dB/km, safely covering the emission spectrum of NE 102A. The manufacturer quotes attenuations between 100 and 300 dB/km in the wavelength range from 400–450 nm. We measured a value of 260 dB/km. A bundle of 16 fibers, densely packed within a flexible and light tight polyethylene tube (outer diameter 2 mm), does not show any cross-talk of light between the fibers. Using such light guides we have bridged distances of up to about 20 m between the radiation source and the PMT.

### C. The photomultiplier tubes

We have used single- and multi-cathode tubes, depending on the dosimetric application. The single-cathode tube was a Hamamatsu photomultiplier R647-01, a ten-stage, head-on PMT with a  $\frac{1}{2}$ " cathode diameter and an overall length of 70 mm. Its spectral sensitivity has a maximum at 420 nm which nicely matches the light emission maximum of NE 102A. For a high voltage of 1000 V the amplification was about  $10^6$  and the dark current about 20–100 pA under normal conditions (without cooling).

In some applications of scintillation dosimeters we used detector arrays which were read out by a 16-channel PMT Hamamatsu R4760. The purchased specimen had amplifications and dark currents similar to those of the single-channel PMT. The cross-talk between the individual channels, however, caused some problems. We measured a mean for our specimen of 0.5%, which is close to the manufacturer's specifications of 0.3%. Such a value would be quite tolerable if all cross-talks were of similar size. However, we found a large spread, with a maximal cross-talk of 4.5%. Therefore, we had to correct the results of the individual channels by an unfolding procedure employing a measured cross-talk matrix. In addition care was taken that channels with large cross-talk (which, unexpectedly, were not always neighbors) did not differ too much in the signal size.

## III. GENERAL PROPERTIES OF SCINTILLATION DOSEMETER SYSTEMS

### A. Construction principles

In all our applications the scintillator probes had small volumes on the order of 1 mm<sup>3</sup> up to 10 mm<sup>3</sup>. The probes have been glued onto the face of the light guide fibers using a cyanoacrylate adhesive (Panacol Elosol cyanolit 202). In all cases where compensation of light background was necessary (Sec. III C) we have used bundles of 8 or 16 fibers. These could be divided into two groups (signal and background) equally distributed over the cross section of the fiber bundle. Each group was read out separately by a PMT (Fig.

1). The scintillator probe together with the end pieces of the light guides were tightly packed together using a light-tight coating, e.g., a thermo-shrinkable tubing or a self-adhesive polyethylene tape (Fig. 1). This material added a 200- $\mu\text{m}$ -thick skin of approximate water equivalence in the case of external beam dosimetry. For special applications the detector was embedded in a block of tissue substituting material, e.g., for  $^{125}\text{I}$  eye-plaque dosimetry (see Sec. IV D).

### B. Properties of scintillation dosimeter systems—typical measurement currents, dose rates, and stability

The measuring currents scale roughly with the volume of the scintillator probe. They depend on the effects of light attenuation (light guide, coupling, etc.) as well as on the PMT quantum efficiency and amplification. A 1- $\text{mm}^3$  scintillator probe with a 20-cm-long light guide yielded a typical measuring current of 5  $\mu\text{A}/(\text{Gy min}^{-1})$  when operating the PMT at 1 kV. If the PMT is continuously kept on high voltage, scintillation dosimeters have been operated for several months with a stability within a few percent.

Scintillation dosimeters have been used at dose rates from about 10  $\mu\text{Gy}/\text{min}$  (ophthalmic plaque dosimetry) to about 10  $\text{Gy}/\text{min}$  (external beam dosimetry). In practice the PMT dark current (see Sec. II B) sets the lower limit to the measurable dose rate. An upper dose rate limit was not reached in our measurements. Theoretically, values up to 20  $\text{Gy}/\text{min}$ , corresponding to a current of 50  $\mu\text{A}$ , should be measured without saturation effects (Photomultiplier tubes, Hamamatsu City, Japan, 1988).

### C. Background corrections

There are three sources of background that have to be taken into account in a scintillation dosimeter system: background light generated in the light guide, PMT dark currents, and radiation-induced PMT currents. The PMT dark currents have to be measured and subtracted from the signal. Radiation-induced PMT currents can be avoided by keeping the tube sufficiently out of the field. Background light can be caused by luminescent excitations or by the Cerenkov effect, which is, by far, the dominating background source for radiation fields containing sufficiently energetic primary or secondary electrons (threshold energy of 170 keV in plastic light guides).<sup>6,7,9–11</sup> The background light was measured simultaneously by blind fibers (see Sec. III A). Both channels were calibrated relatively, then the background signal was subtracted from the scintillator signal.<sup>11,12</sup>

The relative intensity of the background compared to the scintillation light strongly depends on the beam energy and the geometry of the system. For a 10-MV photon beam and a field size of 30 $\times$ 30  $\text{cm}^2$ , for instance, we measured a background contribution up to 15% of the total signal with scintillator volume of 5  $\text{mm}^3$ . Similar results were obtained by Beddar *et al.*<sup>5</sup> In the case of ophthalmic applicators ( $^{125}\text{I}$  and  $^{106}\text{Ru}/^{106}\text{Rh}$  sources), the background light was found to be less than 2% of the scintillation light. Furthermore, background and signal showed the same functional dependences

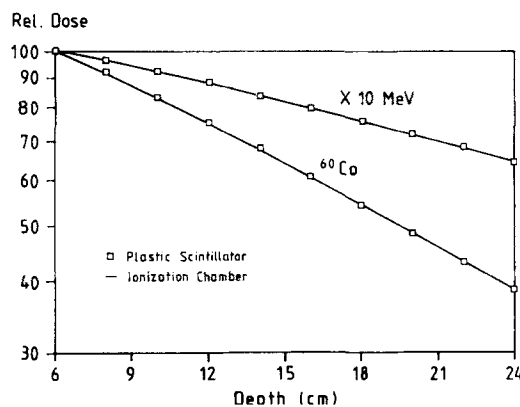


FIG. 3. Comparison of scintillator and ionization chamber (PTW 23332) measurement data at a  $^{60}\text{Co}$  and a 10-MeV photon beam (Ref. 12. The measurement was performed in a solid body phantom made of PVT, the base material of the NE 102A scintillator (complete equivalence of detector and surrounding material).

on the distance to the plaque surface. The effect of background light on the measurement of relative dose distributions could be neglected therefore.

### D. Dose proportionality and fields of application

We have built scintillation dosimeter systems for different applications, including

- (i) interface dosimetry in tissue heterogeneities for the investigation of the dose to lung in total body irradiation with external beams,<sup>11,12,22–24</sup>
- (ii) ophthalmic plaque dosimetry,<sup>22,23,25–27</sup>
- (iii)  $^{192}\text{Ir}$ -afterloading dosimetry.<sup>23,28–30</sup>

For these applications we investigated the dose linearity of the scintillation detector output by comparing the signal to that obtained by a suitable reference detector. As references we used ionization chambers in the case of external beam dosimetry and TLDs for eye plaque dosimetry.

As examples of our measurements a comparison of depth dose curves is shown in Figs. 3–5 for  $^{60}\text{Co}$   $\gamma$  rays, a 10-MeV photon beam, a 17-MeV electron beam, and for an  $^{125}\text{I}$  source. The electron dosimetry was performed in a water

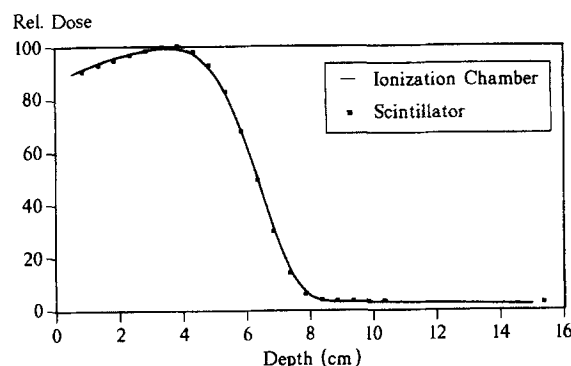


FIG. 4. Comparison of scintillator and ionization chamber (PTW 233641) measurement data at a 17-MeV electron beam measured in water.

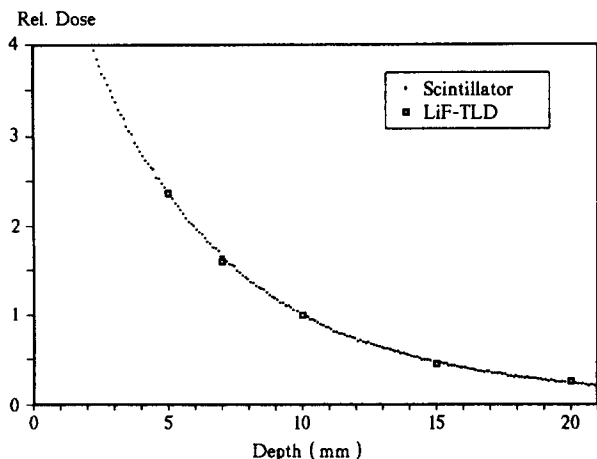


FIG. 5. Comparison of scintillator and LiF-TLD measurement data at the depth dose curve of an  $^{125}\text{I}$  ophthalmic applicator.

phantom while a water-substituting material was used in all cases of photon dosimetry. The curves of the scintillation dosimeter and the reference detector are in good agreement. For the photon dosimetry the values of both detectors agreed within 0.3% ( $^{60}\text{Co}$ ), 0.4% ( $\times 10$  MeV), and 2.3% ( $^{125}\text{I}$ ). The values on the electron depth dose curve agreed within 1.2%, except for the region of the maximal electron range. Here we stated deviations up to some 10%. The use of absolutely measuring dosimeters also allows a stability check and an absolute calibration of the scintillation dosimeter, if necessary.

#### IV. APPLICATION TO OPHTHALMIC PLAQUE DOSIMETRY

##### A. Ophthalmic plaque therapy

At the Essen University Hospital eye plaques with  $^{106}\text{Ru}/^{106}\text{Rh}$  and  $^{125}\text{I}$  are employed for the treatment of intraocular tumors. The ready-to-use ruthenium plaques are delivered by the manufacturer with a certificate (Applicator certificate, BEBIG GmbH, Berlin, Germany, 1991) containing the surface activity distribution and a depth dose rate curve measured up to a maximal depth of 5 mm (Fig. 6). For iodine plaques Amersham seeds type 6702 are used. Some information about the properties and the application of the employed radionuclides is given in Table II.<sup>31</sup>

##### B. 2-D/3-D plaque dosimetry—motivation and first approaches

After the treatment of some 100 patients with plaque type A (Fig. 7), frequently complications have been observed, such as radiation-induced neuropathy of the optical nerve and secondary glaucoma (private communication, Sauerwein, Universitätsklinikum Essen, Germany). There was a suspicion that the dose distribution of these plaques was too broad to assure an efficient sparing of the radiosensitive structures within or close to the eye. Therefore, we have started investigations with the aim of optimizing the applica-

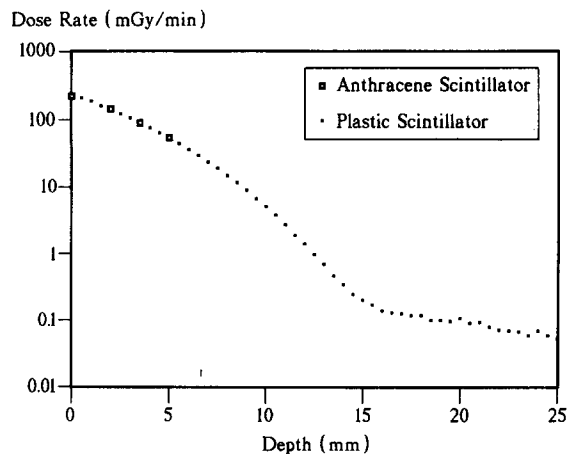


FIG. 6. Comparison of measuring data of the depth dose rate curve of a  $^{106}\text{Ru}/^{106}\text{Rh}$  ophthalmic applicator. The anthracene scintillator measurement is provided by the manufacturer (Applicator certificate, BEBIG GmbH, Berlin, Germany, 1991). The plastic scintillator data are measured by the authors. Note the much steeper gradient of the curve compared to the iodine plaque (Fig. 5).

tors to a better sparing of these structures at risk without reducing the dose in the malignant tissue. The basis for improvements is the determination of fully three-dimensional (3-D) dose distributions within the eye and the neighboring tissues. The required spatial resolution in the millimeter and submillimeter regime could previously only be achieved by very time consuming TLD measurements.

Initially we performed our measurements in a water phantom containing the applicator. A computer-controlled scintillator probe (diameter and length 1 mm) scanned the interesting volume. It was attached via its light guide to an eye tissue substituting fixation pin with 5-mm diameter (RE-1, see Sec. IV D). The determination of a 2-D distribution with about 200 measuring positions ( $1 \times 1\text{-mm}^2$  grid) typically took half an hour. The time necessary for the measurement of a fully three-dimensional dose distribution was in the order of the effort for the plaque preparation: some hours.

##### C. Optimization of ophthalmic plaques

A number of prototype applicators were analyzed to determine the influence of the seed position, the curvature of the calottes, and the shielding of radiation on the dose distribution. Figure 7 shows examples. The applicator B consisted of a gold calotte, a carrier calotte, and an inner mask calotte

TABLE II. Radionuclides used for ophthalmic applicators—radiation energy and dosage scheme at the Essen University Hospital.

Radionuclide	Emitted radiation	Therapeutical application/dosage
$^{125}\text{I}$	$\gamma$ and x rays <sup>27</sup> 20–35 keV	Tumor prominence 5–10 (12) mm 400–700 Gy at the sclera 80–100 Gy at the tumor apex
$^{106}\text{Rh}/^{106}\text{Ru}$	$\beta$ -radiation max. 3.5 MeV $\gamma$ -ray and bremsstrahlung background	Tumor prominence 2–5 (6) mm 700–1000 Gy at the sclera min. 100 Gy at the tumor apex

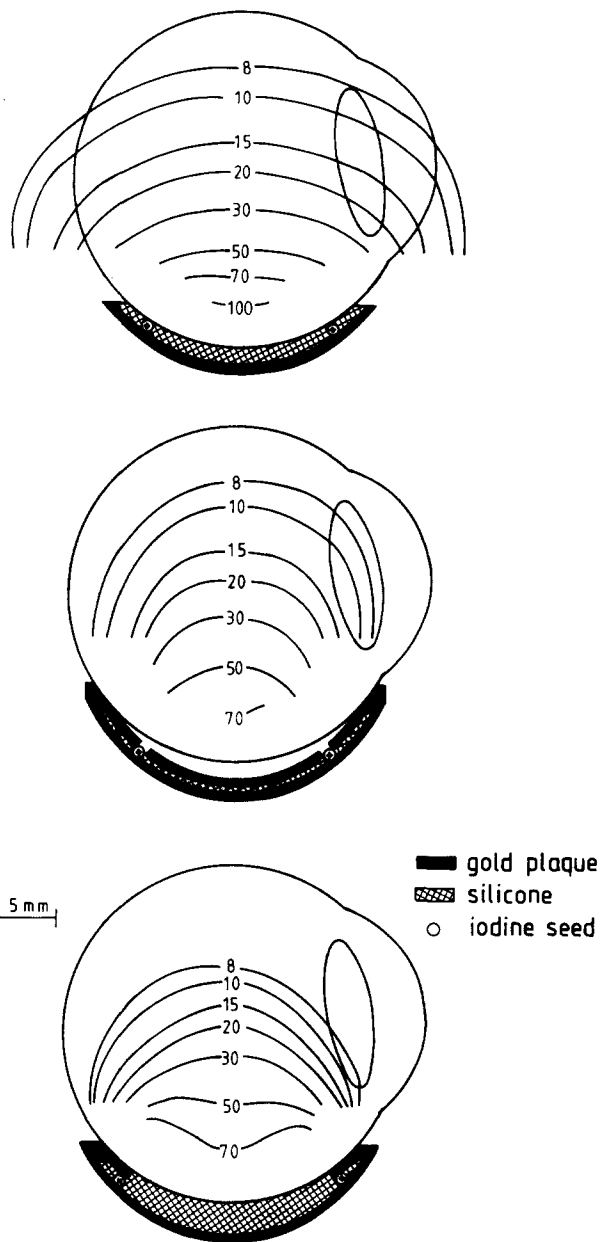


FIG. 7. Comparison of the relative dose distributions of the iodine applicators type A (top), type B (center), and type C (bottom). Normalized to 50 Gy at 7-mm depth.

with slits for the seeds (private communication, Sauerwein, Universitätsklinikum Essen, Germany). The effect of the slits was a focused collimation of the primary radiation and a reduction of the scattered radiation from the carrier calotte. The radius of curvature of the inner calotte was only 10 mm as compared to 12 mm for the type A plaque.

The applicator C was completely different: the seeds were positioned underneath a shielding ring made of gold at the edge of the gold calotte. In this way the primary radiation was partially shielded. Thus, the dose distribution was determined by penumbra effects and secondary radiation. The dose distribution of the types B and C had better defined boundaries than the A type. In addition, the applicator C

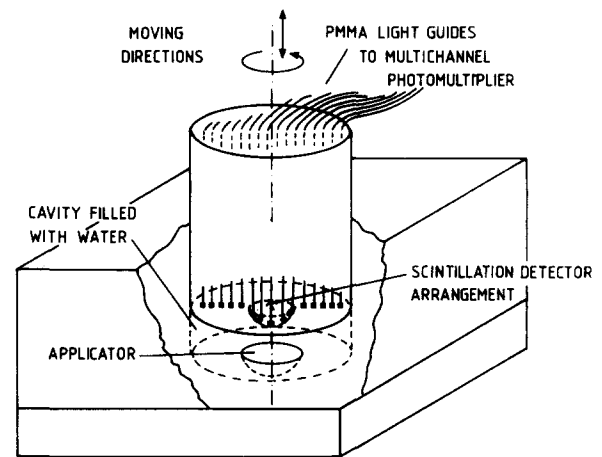


FIG. 8. Diagram of the partially solid eye phantom, including a matrix of 16 scintillation dosimeters read out by a multi-channel PMT.

showed a steeper depth dose curve, a property which supports sparing sensitive structures opposite to the tumor.

## D. A multi-channel dosimeter for 3-D treatment planning

### 1. The detector system

The fast scintillator dosimetry provides a measuring technique for individual dosimetric treatment planning. In order to apply this concept of "dosimetric treatment planning"<sup>26</sup> to the clinical routine, we designed a multi-detector array in a solid body phantom with parallel data acquisition.<sup>25,27</sup> The phantom was made of RE-1, an eye tissue substitute developed by Harder and Herrmann for the dosimetry of low energy photons.<sup>32</sup> The main parts of the phantom are shown in Fig. 8: a basic block with a bore, the applicator at the bottom of the bore, and a cylindrical piston sliding up and down the bore. An array of 16 scintillators was inserted directly at the surface of the piston whose head was shaped according to the eye curvature. All gaps which could influence the dose distribution were filled with water. A vertical movement of the piston allowed us to take a 2-D dose distribution; an additional rotation about the vertical axis a complete 3-D distribution. After a 180° rotation the detectors were located in positions interleaved with those of the 0° position. This improved the spatial resolution by a factor of 2. The spacing of measuring points was 1.4 mm in the radial direction and could be arbitrarily chosen in the axial direction. The signals were measured by a multi-channel PMT and a multi-channel electrometer.

### 2. Calibration, and first results

The 16 detectors had to be calibrated relatively. To avoid positioning errors, we measured a dose distribution in a water phantom with each detector. The measured, interpolated distributions were then matched by a fitting algorithm and normalized to equal dose values by applying the calibration constants. An absolute calibration could be obtained by one additional measurement with a calibrated standard detector.

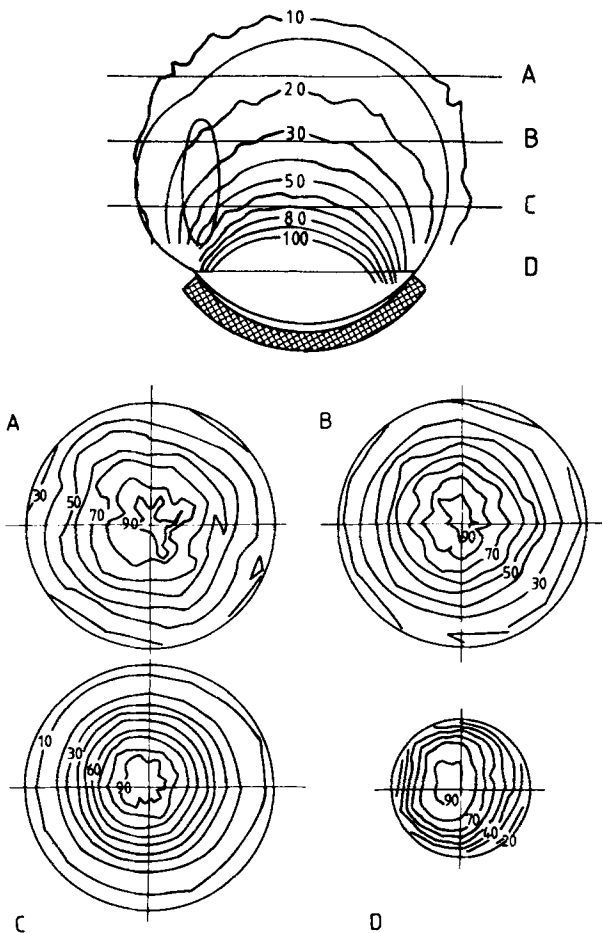


FIG. 9. The 3-D measurement of an iodine plaque with cross section in the vertical direction (normalized to 80 Gy at 8-mm depth) and four cross sections in the horizontal direction (A–D). Plane A–D: dose distribution normalized to the maximum value in each plane (=100%). These measurements show the influence of an asymmetric surface activity distribution on the dose distribution. This influence decreases from short (plane D) to larger distances (plane A), due to increasing scatter contributions to the absorbed dose.

With this multi-channel, parallel readout dosimeter system the measuring time is further reduced by an order of magnitude. A complete 3-D dose distribution of an eye plaque can be obtained in 30–60 min (Fig. 9). This time is comparable to that for a physically correct computer-based eye plaque treatment planning employing Monte Carlo simulations. Thus, our new concept of “dosimetric treatment planning” offers a more direct access to the dose distributions and could complement Monte Carlo methods in many applications.

## V. CONCLUSION

We have developed dosimeter systems based on plastic scintillators as probes for various applications in radiotherapy. In particular, for many notoriously problematic fields of clinical dosimetry, as measurements in fields with steep dose gradients, in regions without secondary electron equilibrium or in fields with mixed radiation beams, this in-

strument offers an ideal solution. Typical fields of application are interface dosimetry in external beam therapy or dosimetry of brachytherapy applicators (afterloading, eye plaques). Scintillators are especially suitable for *in vivo* dosimetry and dose monitor systems. In this paper we have described the favorable properties of plastic scintillator detectors which render them superior to other detector types for such applications.

The most important advantages are

- (i) approximate water/tissue equivalence of scintillators and light guides for all electron energies and photon energies above about 120 keV;
- (ii) high spatial resolution since scintillator probes can be prepared in nearly any size and shape (high sensitivity);
- (iii) a large dynamic range (several orders of magnitude of dose rates can be covered);
- (iv) direct reading of absorbed dose without energy-dependent corrections;
- (v) no temperature or pressure dependence;
- (vi) no dependence on the direction of incidence of the radiation;
- (vii) no significant radiation damage of scintillators used in clinical routine over years, long time stability;
- (viii) no high voltage within the detector volume.

## A. Properties of systems

The scintillation light is transmitted by flexible fibers to small PMTs outside the radiation field. Background light generated in the light guide can simultaneously be measured and subtracted. With the use of multi-cathode PMTs, detector arrays can be read out in parallel. A computer-controlled multi-channel system allows a 3-D scan, e.g., of an eye plaque, within about one hour. Thus, a dosimetric optimization of applicators is possible, achieving a much better sparing of organs at risk.

## B. Possible improvements

The development of multi-channel PMTs with more channels and reduced cross-talk will offer improved conditions for simultaneous measurements in the future. Unlike film or TLD dosimetry, such a system will allow an on-line measurement. Therefore, it is suitable also for the quality control and *in vivo* dosimetry at radiation units with dynamic irradiation techniques.<sup>23</sup>

## ACKNOWLEDGMENTS

These investigations were partly supported by grants of the Deutsche Forschungsgemeinschaft (DFG), the German Research Foundation. The authors wish to thank Dr. K.-P. Herrmann and Prof. Dr. D. Harder, Göttingen/Germany, for their help in designing and constructing the ophthalmic plaque dosimetry phantom based on RE-1.

- <sup>1</sup>L. L. Meisberger, R. J. Keller, and R. J. Shalek, "The effective attenuation of the gamma rays of Gold 198, Iridium 192, Cesium 137, Radium 226, and Cobalt 60," *Radiology* **90**, 953–957 (1968).
- <sup>2</sup>F. O'Foghluha, "Scintillation dosimetry and an application of it," *Ann. NY Acad. Sci.* **161**, 86–93 (1969).
- <sup>3</sup>H. Schmidt, "Zur Beta-Dosimetrie medizinischer Applikatoren," *Isotopenpraxis* **13**, 413–418 (1977).
- <sup>4</sup>A. S. Beddar, T. R. Mackie, and F. H. Attix, "Water-equivalent plastic scintillation detectors for high-energy beam dosimetry: I. Physical characteristics and theoretical considerations," *Phys. Med. Biol.* **37**, 1883–1900 (1992).
- <sup>5</sup>A. S. Beddar, T. R. Mackie, and F. H. Attix, "Water-equivalent plastic scintillation detectors for high-energy beam dosimetry: II. Properties and measurements," *Phys. Med. Biol.* **37**, 1901–1913 (1992).
- <sup>6</sup>M. Heintz, D. Flühs, U. Quast, H. Kolanoski, and St. Reinhardt, "Dosisbestimmung bei der Ganzkörperbestrahlung—Dosimetrische Konzepte und Monte-Carlo-Rechnungen," Tagungsband DGMP, *Medizinische Physik* **92**, edited by J. Roth (Basel, 1992), pp. 86–87.
- <sup>7</sup>A. S. Beddar, F. H. Attix, and T. R. Mackie, "On the nature of the light induced by radiation in transparent media used in radiotherapy," *Med. Phys.* **16**, 683 (1989) (abstract).
- <sup>8</sup>C. M. Meger Wells, T. R. Mackie, M. B. Podgorsak, M. A. Holmes, N. Papanikolaou, P. J. Reckwerdt, J. Cygler, D. W. O. Rogers, A. F. Bielajew, D. G. Schmidt, and J. K. Muehlenkamp, "Measurements of the electron dose distribution near inhomogeneities using a plastic scintillation detector," *Int. J. Radiat. Oncol. Biol. Phys.* **29**, 1157–1165 (1994).
- <sup>9</sup>A. S. Beddar, T. R. Mackie, and F. H. Attix, "Cerenkov light generated in optical fibers and other light pipes irradiated by electron beams," *Phys. Med. Biol.* **37**, 925–935 (1992).
- <sup>10</sup>S. F. de Boer, A. S. Beddar, and J. A. Rawlinson, "Optical filtering and spectral measurements of radiation-induced light in plastic scintillation dosimetry," *Phys. Med. Biol.* **38**, 945–958 (1993).
- <sup>11</sup>D. Flühs, *Aufbau und Einsatz eines Szintillationsdetektorsystems zur Messung von Dosisverteilungen an einem <sup>60</sup>Co-Teletherapiegerät* (Diplomarbeit Universität, Dortmund, 1989). Free copies of thesis are available and may be obtained from Dipl.-Phys. D. Flühs, c/o Universität Dortmund, Institut für Physik, Otto-Hahn-Str. 4, D-44221 Dortmund, Germany.
- <sup>12</sup>M. Heintz, *Einflüsse von Detektoren bei der Dosismessung in Gewebehomogenitäten* (Diplomarbeit Universität, Dortmund, 1992).
- <sup>13</sup>ICRU Report 37, *Stopping Powers for Electrons and Positrons* (ICRU, Bethesda, MD, 1984).
- <sup>14</sup>J. H. Hubbell, "Photon mass attenuation and mass energy absorption coefficients for H, C, N, O, Ar, and seven mixtures from 0.1 keV to 20 MeV," *Radiat. Res.* **70**, 58–81 (1977).
- <sup>15</sup>J. H. Hubbell, "Photon mass attenuation and energy-absorption coefficients from 1 keV to 20 MeV," *Int. J. Appl. Radiat. Isot.* **33**, 1269–1290 (1982).
- <sup>16</sup>R. L. Craun and D. L. Smith, "Analysis of response data for several organic scintillators," *Nucl. Instrum. Methods* **80**, 239–244 (1970).
- <sup>17</sup>B. Brannen and G. L. Olde, "The response of organic scintillators to electron energy deposited in them," *Radiat. Res.* **16**, 1–6 (1962).
- <sup>18</sup>D. L. Horrocks, *The Current Status of Liquid Scintillation Counting*, edited by E. D. Bransome, Jr. (Grune and Stratton, New York, 1970).
- <sup>19</sup>H.-H. Kausch-Blecken von Schmeling, "Die Lichtausbeute organischer Szintillatoren für Elektronen von 1 bis 12 keV," *Z. Phys.* **160**, 520–526 (1960).
- <sup>20</sup>A. J. Meyerott, P. C. Fisher, and D. T. Roethig, "Plastic scintillator response to 1–10 keV photons," *Rev. Sci. Instrum.* **35**, 669–672 (1964).
- <sup>21</sup>M. Kaiser, *Untersuchungen zur Strahlenschädigung in organischen Szintillatoren und szintillierendem Glas* (Diplomarbeit Universität, Dortmund, 1986). Free copies of thesis are available and may be obtained from Dipl.-Phys. D. Flühs, c/o Universität Dortmund, Institut für Physik, Otto-Hahn-Str. 4, D-44221 Dortmund, Germany.
- <sup>22</sup>D. Flühs, M. Heintz, F. Indenkämpen, C. Wieczorek, H. Kolanoski, and U. Quast, "Ein neues Dosimetrie-Konzept: energie- und richtungsunabhängige, hochauflösende, schnelle 2D und 3D-Dosimetrie mit Plastikszintillatoren," Tagungsband DGMP *Medizinische Physik* **93**, edited by R. G. Müller and J. Erb (Erlangen, 1993), pp. 366–367.
- <sup>23</sup>U. Quast, D. Flühs, and H. Kolanoski, "A general concept of dosimetry ideal for advanced radiotherapy techniques like TBI, ISER, IORT, conformal or brachytherapy," in *Proc. International Congress Advanced Diagnostic Modalities and new Irradiation Techniques in Radiotherapy*, edited by G. Gobbi and P. Latini (Perugia, 1994), pp. 179–186.
- <sup>24</sup>U. Quast, D. Flühs, and H. Kolanoski, "Clinical dosimetry with plastic scintillators - almost energy independent, direct absorbed dose reading with high resolution," in *Proc. IAEA Radiotherapy Dosimetry: Radiation Dose in Radiotherapy from Prescription to Delivery*, IAEA-SR-188 (1994), p. 37.
- <sup>25</sup>D. Flühs, M. Heintz, C. Wieczorek, A. Wiescholke, H. Kolanoski, and U. Quast, "Plastikszintillationsdetektor - schnelle 3D-Dosimetrie für die Bestrahlungsplanung von <sup>125</sup>I und <sup>106</sup>Ru/<sup>106</sup>Rh-Augenapplikatoren," Tagungsband DGMP *Medizinische Physik* **93**, edited by R. G. Müller and J. Erb (Erlangen, 1993), pp. 358–359.
- <sup>26</sup>D. Flühs, U. Quast, H. Kolanoski, and M. Heintz, "Dosimetric treatment planning-fast 2D/3D-dosimetry," *Proc. XIth ICCRT, Manchester*, (1994), pp. 38–39.
- <sup>27</sup>C. Wieczorek, *Aufbau eines Mehrkanal-3D-Dosimetriesystems basierend auf Plastikszintillatoren zur Anwendung in der Augentumorthherapie* (Diplomarbeit Universität, Dortmund, 1994). Free copies of thesis are available and may be obtained from Dipl.-Phys. D. Flühs, c/o Universität Dortmund, Institut für Physik, Otto-Hahn-Str. 4, D-44221 Dortmund, Germany.
- <sup>28</sup>U. Quast, D. Flühs, M. Heintz, F. Indenkämpen, and H. Kolanoski, "Tissue equivalent plastic scintillator probes: Fast, precise <sup>192</sup>Ir-afterloading dosimetry. Principles and clinical application," *GEC-ESTRO-Meeting, Linz, Radiother. Oncol.* **31** (Suppl. 1), 22 (1994) (abstract).
- <sup>29</sup>D. Flühs, F. Indenkämpen, M. Heintz, H. Kolanoski, and U. Quast, "Tissue equivalent plastic scintillator probes: Fast, precise <sup>192</sup>Ir-afterloading dosimetry. Dosimetric treatment planning and verification," *GEC-ESTRO-Meeting, Linz, Radiother. Oncol.* **31** (Suppl. 1), 26 (1994) (abstract).
- <sup>30</sup>U. Quast, D. Flühs, and F. Indenkämpen, "The built-in dose monitor. A new dosimetric concept for afterloading quality assurance," *Radiother. Oncol.* **32** (Suppl. 1), 30 (1994).
- <sup>31</sup>C. C. Ling, E. D. Yorke, I. J. Spiro, D. Kubiatowicz, and D. Bennett, "Physical dosimetry of <sup>125</sup>I seeds of a new design for interstitial implant," *Int. J. Radiat. Oncol. Biol. Phys.* **9**, 1747–1752 (1983).
- <sup>32</sup>K.-P. Herrmann, W. Alberti, P. Tabor, B. Pothmann, St. Divoux, and D. Harder, "Solid phantom material for the dosimetry of iodine-125 seed ophthalmic plaques," *Int. J. Radiat. Oncol. Biol. Phys.* **26**, 897–901 (1993).